ISESCO JOURNAL of Science and Technology
Volume 8 - Number 13 - May 2012 (67-74)

CFD Analysis of a Two-bucket Savonius Rotor for Various Overlap Conditions

Rajat Gupta[1], Ranjan Das[2], Rituraj Gautam[3], Siddhartha Sankar Deka[3]

[1]Professor, Department of Mechanical Engineering, National Institute of Technology Silchar, Silchar, Assam, PIN-788010, India

[2]Assistant Professor, Department of Mechanical Engineering, Tezpur University, Tezpur, Assam, PIN- 784028, India

[3]8th Semester Undergraduate Students in Mechanical Engineering, National Institute of Technology Silchar, Silchar, PIN-788010, India

Email: ssdeka.nits@gmail.com

Abstract

Savonius turbine, a Vertical Axis Wind Turbine (VAWT), is self-starting, Omni-directional, and has high starting torque. In this paper, an attempt was made to study the flow behaviour (static pressure and velocity contours) of a rotating two-bucket Savonius rotor using Computational Fluid Dynamics. CFD analysis was carried out to model the complex flow physics around the rotating rotor, as it consumes less time and computational cost. For this purpose, data were taken from the experiments conducted earlier on the rotor in a subsonic wind tunnel for five overlap conditions, namely 16.2%, 20%, 25%, 30% & 35%. The rotor was 20cm in height and the buckets were 8 cm in diameter. A two-dimensional computational unstructured mesh (triangular mesh) model was developed for the rotor in Gambit 2.3.16 package of Fluent 6.3.26 software. A k-ε turbulence closure model with standard wall treatment function was selected. A second order upwind discretization scheme was adopted for pressure velocity coupling of the flow. The sequential algorithm, Semi-Implicit Method for Pressure-Linked Equation (SIMPLE) was used for solving all the scalar variables. The flow was simulated under steady-state condition, and the single rotating reference frame (MOVING WALL) was considered for the buckets. From the simulations done in Fluent 6.3.26 software, the flow patterns through the rotating rotor at 00 rotor angle for the above overlap conditions were analyzed with the help of static pressure and velocity contours. The pressure drop across the rotor from upstream to downstream side was the maximum in case of 16.2% overlap indicating maximum power extraction from the wind at that overlap condition. Vortices formed on the concave side of the advancing bucket due to flow separations from adverse pressure gradient were less up to 16.2% overlap, which increased with higher overlaps leading to reduction in positive torque by the advancing bucket. Moreover, for 16.2% overlap, maximum pressure difference was obtained across the returning bucket, thereby increasing the overall aerodynamic torque and power for the rotor.

Keywords: *CFD,Pressure Contours, Savonius rotor, Velocity Vectors.*

1. Introduction

Wind energy is the kinetic energy associated with the movement of atmospheric air from a region of high pressure to a region of low pressure. The pressure variation caused due to rotation of earth and uneven heating have an effect on the surface of the earth. Wind turbine is a type of a device used for extraction of wind energy and converting it into mechanical energy. The extraction of mechanical power from the wind is an ancient practice dating back to at least 3000 years. Beginning with sailing ships, the technical insight gained from them was extended to the early windmills

for grinding of corn, irrigation purposes, pumping of water from wells etc. Even today, wind energy is used to generate electricity to provide electrification into rural areas and other far-fetched locations. Windmills believed to have originated in Persia in the seventh century and gradually spread to Europe in the twelfth century. The design gradually improved, especially in England during the eighteenth century, where millwrights developed remarkably effective self-acting control mechanisms. Wind energy has been growing rapidly in recent years. Wind energy is relatively cheap, it is scalable, and a single wind turbine can generate a lot of power. Some other advantages of wind energy are that it has led to reduction in the use of fossil fuels, leading to a reduction in the emission of toxic gas pollutants (the most important of these being the oxides of carbon, sulphur and nitrogen). It is fast becoming an international business sector, spreading beyond its original markets in a few European countries, India and United States. The annual market of wind energy continues to grow at an astonishing rate of 32%[1]. It is predicted by Greenpeace that 10% of the required electricity generation could be provided by wind energy by the year 2020, added with improved technology along with superior economics, wind energy could capture 5% of the world energy market by the year 2020[2]. The major manufacturers and project developers of wind energy systems now operate across all five continents. A large number of operational onshore wind farms are located in the USA. The Roscoe Wind Farm is the largest onshore wind farm in the world at 781.5 MW, followed by the Horse Hollow Wind Energy Center at 735.5 MW[3]. Also the Thanet Offshore Wind Project in United Kingdom is the largest offshore wind farm in the world having a combined wind energy production of 300 MW followed by Horns Rev II of 209 MW generating capacity in Denmark[4]. According to the figures released by Global Wind Energy Council (GWEC), wind energy developing countries (more than 70) have taken the net wind energy installed capacity to a record high of 742,223MW[5].In developing countries like India where the energy consumption is increasing day-by-day; large-scale wind farms like these can play a generous role. India has an installed capacity of about 11807.00 MW in wind energy sector as on March 31, 2010[6]. In terms of wind power installed capacity, India ranks 5th in the world.

Wind turbines are classified into two types, based on the type of orientation of the axis of rotation of the blades. They are VAWT (Vertical Axis Wind Turbine) and HAWT (Horizontal Axis Wind Turbine). In this paper, the type of VAWT that we are considering is a two-bucket Savonius rotor. Sigurd J. Savonius invented the Savonius rotor in the year 1922. When viewing the rotor from above, it appears in the shape of "S" in cross section. The rotor is formed by cutting a cylinder along a central plane and then moving the two semicircular surfaces sideways along the cutting plane. Savonius rotors are different from traditional HAWT_s in that their main axis is perpendicular to the ground. A Savonius rotor scores over a traditional HAWT in areas when it comes to construction, inexpensiveness, high reliability, high starting torque (Blackwell[7]) and its ability to accept wind from any direction. Unlike a traditional HAWT, it is self-starting & hence no mechanism is needed to turn the Savonius rotor towards the wind meaning better performance in areas where a tall tower is not feasible, obstacles are nearby, or the wind is more turbulent. A Savonius rotor is better able to harvest turbulent airflow found around buildings and other obstacles. The two-buckets of a Savonius rotor experience less drag when moving against the wind than moving along with the wind. The differential drag causes the rotor to spin. Being a drag type of device, the power extraction capacity of a Savonius rotor is less as compared to any other VAWT. A Savonius rotor can be particularly productive when it comes to meeting the energy requirements of developing countries. In remote regions of India, there are still places where electricity supply is very much irregular. In those areas, the Savonius rotor can play a vital role for small-scale electricity generation for household applications, drawing water from wells into the agricultural land, milling grains and lots more.

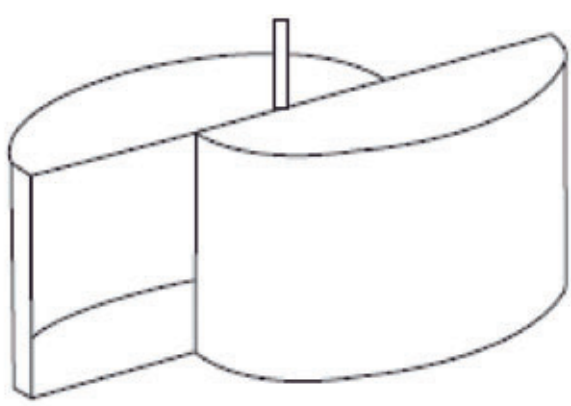

Figure 1. *A two-bucket Savonius rotor showing overlap condition.*

Over the past few decades, a lot of effort has been put by researchers to increase the efficiency of the Savonius rotor [8-19]. Savonius had tested more than 30 models in natural wind and also in open air. He reported the best model had an efficiency of 31% while the maximum reported efficiency of the prototype was 37%. Bach[8] also made some investigations on the Savonius rotor and reported the maximum efficiency of his model as 24%. However, Savonius[20] found that Cp at an overlap ratio of 0.25 is nearly three times than at without overlap condition. In addition, Bach[8] obtained maximum Cp in the overlap range of 0.2-0.25. Khan[11] tested his Savonius rotor in a wind tunnel having provision for overlap variations and reported a highest Cp of 0.375, for blade profile of S-section Savonius rotor at an optimum overlap ratio of 0.30. Blade profiles considered by Khan were semi-circular, NACA aerofoil, double rotor, inverted "S" and non-inverted "S" sections. Aldos[21] made an attempt to augment the power of the Savonius rotor by allowing the blades to swing back when in upwind direction and was successful in achieving a power augmentation of 11.25 with increase in CP from 0.015 to 0.17. He also found that different power augmentation might be achieved with different rotor configurations. Sabzevari[22] made an attempt to improve the performance of a split S-Savonius rotor using ducting's, concentrators and diffusers. He attained a 40% increase in efficiency by using a circularly ducted Savonius rotor equipped with a number of identical wind concentrators and diffusers along the periphery of circular housing. In addition performance tests of two and three-bucket Savonius rotors under different design conditions of the Savonius rotor were performed by different researchers[23-28].

A comparative study of experimental and CFD data was carried out by Gupta et al.29 for power coefficients etc and these two results were seen to be in agreement with minimal error. In this paper, an attempt was made to study the pressure and velocity contours in and around the Savonius rotor (as studied by Gupta *and Das* 2009[29]) for various overlap conditions. The entire analysis was carried out in Fluent 6.3.26 software. For this purpose, input data were taken from the experiments conducted earlier on the rotor in a subsonic wind tunnel, available in the department, for five overlaps, namely 16.2%, 20%, 25%, 30% & 35%.

2. Physical Model of the Savonius Rotor

The model of the Savonius rotor was a two-bucket system having the shape of "S" in cross-section. The model had the provision of changing the overlap ratios, X/D (***Figure 2(a)***), using nut and bolt arrangement. The overlap ratio was varied within 16.2% to 35%. The dimensions of the physical model were 20 cm in height and 8 cm in diameter (***Figure 2(b)***). The thickness considered for the bucket was 5 mm. The experimental model of the rotor was tested in an open circuit wind tunnel present in the department. And the input data for the present study were taken from the experimental data. A brief description of the wind tunnel, experimental procedure utilized and results can be obtained from paper[30].

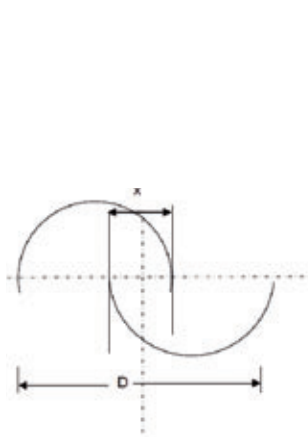

(a) Concept of overlap

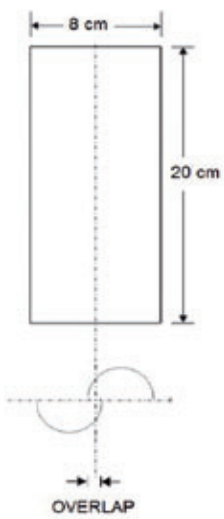

(b) Two Dimensional model of the rotor showing the overlap condition

Figure 2. *A Savonius Rotor showing the overlap condition.*

3. Computational Domain and Boundary Conditions

A two-dimensional view of the rotor model was considered. It is because the buckets rotate in the same plane as the approaching wind. The computational domain shown in the above ***Figure 3*** was the top view of four boundaries of the wind tunnel test section along with physical model of the rotor. The computational domain was discretized using two-dimensional unstructured mesh (triangular mesh). The left boundary had Velocity Inlet condition while the right boundary had Outflow condition. The top and bottom boundaries for the wind tunnel sidewalls had Symmetry conditions. The moving wall condition was employed for the rotor model to study the

effect of fluid motion in and around the rotating Savonius rotor. The dimensions of the computational domain were 100 cm in length and 30 cm in width, which were also similar to the experimental conditions. For the various overlap conditions, the geometry of the rotor was changed and accordingly different meshes were generated for each condition.

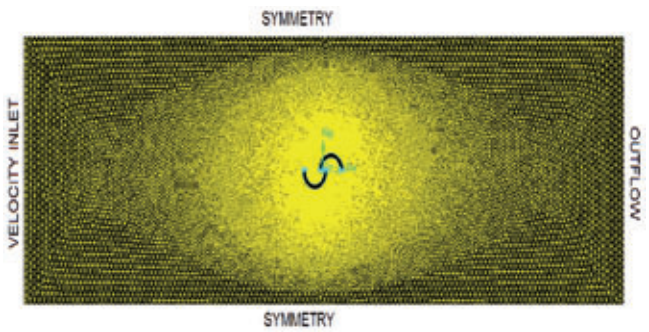

Figure 3. *Physical model, boundary conditions and computational domain of the Savonius rotor at 16.2 overlap condition.*

4. Solution Specifications

1. Solver:

- Solver: Pressure Based
- Time: Steady
- Space: 2D

2. Viscous Model:

- Model: Standard k-epsilon (k-ε)
- Near-Wall Treatment: Standard Wall Functions

3. Material:

Air (μ = 1.7894x10-5 kg/m-s, ρ = 1.225 kg/m3)

4. Operating conditions:

Atmospheric Pressure (1.0132 bar)

5. Boundary Conditions:

- Inlet: Velocity Inlet
- Sides: Symmetry
- Buckets: Moving Wall
- Outlet: Outflow

6. Solution controls:

- Pressure Velocity Coupling: SIMPLE
- Discretization: Momentum (Second Order Upwind), Pressure (Standard)

7. Inlet Velocity: 28 m/s

5. Grid Independence Test

With the increase in the number of triangular cells in the two-dimensional unstructured mesh, the accuracy of the results increases. However, this dependency of the results on the grid is effective up to a certain limit of grid size. No variation in results is observed after that limit with the further increase of grid density. This limit is called the Grid Independent Limit (GIL). In order to obtain GIL condition, Cd was considered as the test para-meter and grid refinements were carried out until a steady value of Cd was obtained. ***Table 1*** shows the various levels of refinement that were considered.

TABLE 1. Various refinement levels considered with the increase in number of nodes.

Refining level	No. of nodes	No. of cells (triangular)
1	11661	22924
2	13449	26484
3	13796	27128
4	17106	33770
5	18124	35798
6	20598	40680
7	23000	45518
8	29719	58916
9	31223	61916
10	32733	64878
11	34120	67644
12	38589	76612

Each level was solved with same input parameters in Fluent 6.3.26. The ***Figure 4*** shows the variation of the Cd values with the no of nodes. The refinement level 10 was considered for the final simulation.

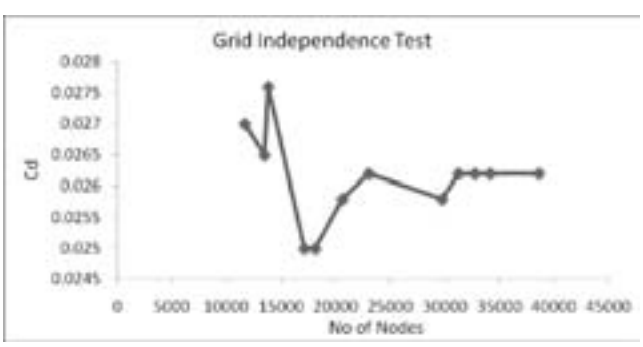

Figure 4. *Grid independence test carried out for a two-bucket S rotor.*

6. Velocity Vectors and Pressure Contours Analysis for Various Overlap Conditions

Figure 5. *Pressure contour for 16.2% overlap.*

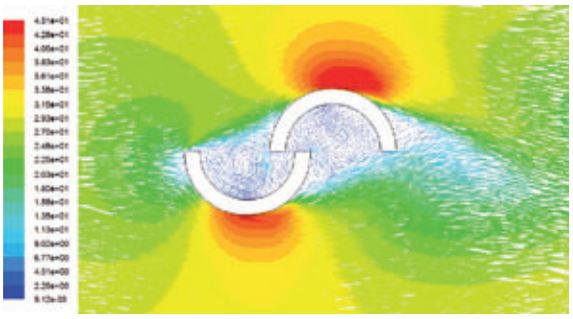

Figure 6. *Velocity contour for 16.2% overlap.*

Figure 7. *Pressure contour for 20% overlap.*

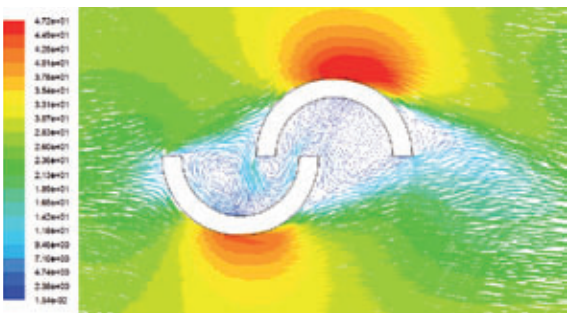

Figure 8. *Velocity contour for 20% overlap.*

Figure 9. *Pressure contour for 25% overlap.*

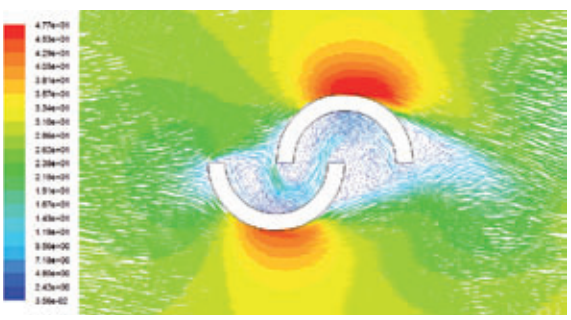

Figure 10. *Velocity contour for 25% overlap.*

Figure 11. *Pressure contour for 30% overlap.*

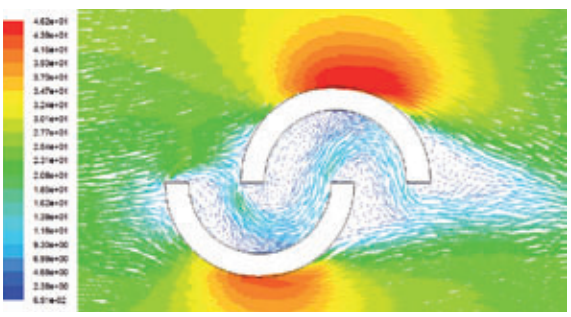

Figure 12. *Velocity contour for 30% overlap.*

Figure 13. *Pressure contour for 35% overlap.*

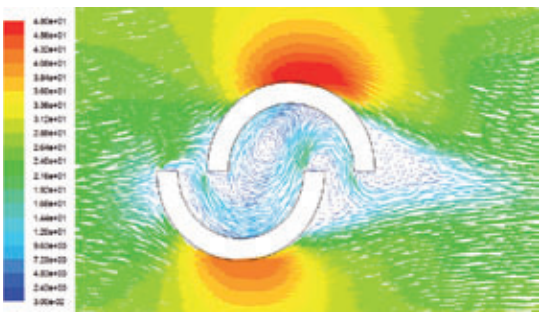

Figure 14. *Velocity contour for 35% overlap.*

The velocity & static pressure contours for the rotating two-bucket Savonius rotor with 00 rotor angle and with various overlaps were analyzed using Fluent 6.3.26 software. In the contour plots, the bucket on the left hand side is the returning bucket and that on the right hand side is the advancing bucket. The contour plots predict the variations in velocity and pressure in various regions near the buckets within the flow domain. It can be observed from the pressure contour plots that pressure drop occur across the rotor from upstream to downstream side. This pressure drop indicates power extracted by the rotor causing its rotation[31]. The maximum static pressure drop is found in case of rotor with 16.2% overlap (18.41e+02 Pa) figure 5 and minimum in case of rotor with 35% overlap (9.27e+02 Pa) ***Figure 13***. Thus maximum power extraction occurs in case of rotors with 16.2% overlap which decreases with subsequent increase in overlap. This is fairly in agreement with the findings made by Newman[16] and Shankar[32]. The static pressure on the convex side of both the buckets can be observed to be lower than those on the concave side of the buckets; in fact, a region of negative pressure exists on the convex side of the buckets. This occurs due to the high flow velocity over the convex side of the buckets. As a result, a pressure difference acts across the concave and convex side of the buckets, which provide the necessary torque for causing rotation of the buckets. However, it is also observed that the negative pressure produced on the convex side of the buckets is altered with increase in overlap and it tends to increase with further increase in overlap. Further, the pressure difference across the concave and convex faces of the returning bucket is found to be maximum in case of rotor with 16.2% overlap (1.013e+03 Pa), ***Figure 5***, and minimum in case of 35% overlap (2.86e+02 Pa), ***Figure 7***. A phenomenon similar to jet impingement takes place for low overlap of 16.2%, which increases the pressure acting on the concave side of the returning bucket significantly. This increase in pressure on the concave side of the returning bucket increases the aerodynamic torque responsible for rotation of the buckets and thereby enhances overall power extracted by the rotor at that overlap condition. However, the net pressure acting on the advancing and returning buckets comes out to be almost equal in case of 16.2% overlap, (1.027e+03 Pa) in advancing bucket and (1.013e+03 Pa) in returning bucket. Because of this, stability will be obtained in case of 16.2% overlap and hence it will have minimum vibration during rotation. Moreover, the pressure at the tip of the returning bucket is abnormally high, maximum for 35% overlap at 4.41e+02 Pa (***Figure 13***), and minimum for 16.2% overlap at 1.98e+02 Pa (***Figure 5***). Because of this, vibrations in the rotor would occur for overlaps greater than 16.2%, and hence reduce rotor's efficiency.

From the velocity vectors plots, it is seen that vortices are formed on the concave side of the advancing and returning buckets of the Savonius rotor due to flow separation from adverse pressure gradient. The vortices formed on the concave side of the returning bucket gradually diminish with the increase in overlap as shown in ***Figures 8*** & ***10***. This decrease in vortices is due to an increase in flow through the overlap as the overlap increases. However, vortices on the tip of the advancing bucket gradually shift towards the concave side of the advancing bucket with increase in overlap where it grows in size (***Figures 12*** & ***14***), which will lead to the reduction in positive torque by the advancing bucket. Velocity vectors further show that the velocity magnitude on the concave side of both the advancing and returning buckets is less than that on the convex side. This is in agreement with the observation of pressure being higher on the concave side than on the convex side of both the buckets. In addition, the velocity upstream of the rotor is higher than the velocity downstream of the rotor. The velocity difference between upstream and downstream of the flow is found to be the maximum for 16.2 % overlap (4.5e+00 m/s).

Conclusion

In this paper, CFD analysis of a rotating two-bucket Savonius rotor with 00 rotor angle for five overlaps, namely 16.2%, 20%, 25%, 30% & 35% was carried out using Fluent 6.3.26 software. Velocity and static pressure contours were generated for each overlap condition and then these were analysed. From the present study, the following conclusions are summarized:

1) Static pressure decreases from upstream to downstream side of the rotor. The maximum pressure drop is found in case of 16.2% overlap (18.41e+02 Pa) and minimum in case of 35% overlap (9.27e+02 Pa) meaning maximum power extraction from wind by the rotor at 16.2% overlap condition.

2) The pressure difference across the returning bucket is the maximum for 16.2% overlap (1.013e+03 Pa) meaning increase in aerodynamic torque production by the rotor and hence overall power extracted by the rotor at that overlap condition.

3) Velocity vectors show vortices are formed on the concave side of the advancing bucket, which are less up to 16.2% overlap, but increases with higher overlaps leading to the reduction in positive torque by the advancing bucket.

4) The net pressure on the advancing and returning buckets comes out to be almost equal in case of 16.2% overlap (about 1.02e+03 Pa), which would ensure stability of the rotor at 16.2% overlap by minimizing vibration during rotation.

Acknowledgement

The authors acknowledge with thanks the assistance rendered by Dr. Agnimitra Biswas, (Lecturer, Department of Mechanical Engineering, National Institute of Technology Silchar) for providing crucial insights during the course of the research work.

References

[1] G.M.J Herbert, A review of wind energy technologies, Renewable and sustainable energy reviews. Renew Sustain Energy 2007; 11:1117-45.

[2] Global wind energy market as of 2006. Press release of Global Wind Energy Council (GWEC).

[3] Wind Farm: http://en.wikipedia.org/wiki/Wind_farm

[4] Global wind energy market as of 2008. Press release of Global Wind Energy Council; (GWEC), October 2008

[5] G.M. Joselin Herbert, A review of wind energy technologies, Renewable and sustainable energy reviews. Renew Sustain Energy Rev 2007; 11:1117-45.

[6] Indian Wind Energy Association: http://www.inwea.org/

[7] B.F.Blackwell, Wind tunnel performance data for two- & three-bucket Savonius rotor, Sandia Laboratories, Sand 76-0131 under act AT/29-11 1978; 789.

[8] G.Bach, Investigation concerning Savonius rotors and related machines, Translated into English by Brace Research Institute, Quebec, Canada, 1931.

[9] R.B.Macpherson, MSc thesis, University of Massachusetts, Amherst, MA, 1972.

[10] B.G. Newman, Measurement on a Savonius rotor with variable gap, Proceeding of sherbrook. Sherbrook, Canada: University Symposium on Wind Energy; 1974 [p. 116].

[11] M.H.Khan, Model & prototype performance characteristics of S-rotor wind mills, J Wind Eng 1988; 12:59-75.

[12] M.H.Khan, MS thesis, University of the Phillipines, Lasbonas, 1975.

[13] V.J.Modi, Optimal configuration studies and prototype design of a wind energy operated irrigation system, J Wind Eng Ind Aerodyn1984;16:85-96.

[14] U.K.Saha, M.Rajkumar, On the performance analysis of Savonius rotor with twisted blades, J Renew Energy 2005:0960-1481.

[15] V.J.Modi, M.S.U.K. Fernando, On the performance of the Savonius wind turbine, ASME J Solar Eng 1989;11:71-6

[16] B.G.Newman, Measurements on a Savonius rotor with variable gap, Sherbrooke University Syrup. On Wind Energy, 1974.

[17] A.S.Grinspan, Design, development & testing of Savonius wind turbine rotor with twisted blades, In: Proceedings of the 28th national conference on fluid mechanics and fluid power, 13-15 December, Chandigarh, 2001. p. 428-31.

[18] P.N.Shankar, Development of vertical axis wind turbine, Proc Indian Acad Sci 1979;C2(1):49-66. Saylers AT. Blade configuration optimization & performance characteristics of a simple Savonius rotor. Proc Inst Mech Eng 1985;199:185-91.

[19] P.N.Shankar, Development of vertical axis wind turbine. Proc Indian Acad Sci 1979;C2(1):49-66.

[20] S.J. Savonius, The S-rotor and its application, Mech Eng 53, 1931.

[21] T.K.Aldos. Savonius rotor using swinging blades as an augmentation system. J Wind Eng 1984;8(4):214-20.

[22] A.Sabzevari, Power augmentation in a ducted Savonius rotor, In: Second international symposium on wind energy systems, 3-6 October, 1978.

[23] A.J. Alexander, Wind tunnel test on a Savonius rotor. J Ind Aerdyn 1978;3:343-51.

[24] Gavalda Jna, Experimental study on a self adapting Darrieus- Savonius wind machines. J Sol Wind Technol 1990;7(4):457-61.

[25] R.Gupta, R.Das, K.K.Sharma, Experimental study of a Savonius- Darrieus wind machine, In: Proceedings of the international conference on renewable energy for developing countries, 2006.

[26] T. Wakui, (Member Waseda University: /twakui@aoni.waseda.jpS). Hybrid configuration of Darrieus & Savonius rotors for stand-alone wind turbine-generator system.

[27] G.J.M.Darrieus, Turbines having its rotating shaft transverse to the flow of the current. US patent no. 1 835 018, 1931.

[28] A.T. Saylers, Blade configuration optimization & performance characteristics of a simple Savonius rotor, Proc Inst Mech Eng 1985;199:185-91.

[29] R.Gupta, B.K. Debnath, R. Das, CFD analysis of two-bucket Savonius rotor using fluent package, European Wind Energy Conference and Exhibition 2009, Marseille, France.

[30] R.Gupta, A.Biswas, K.K.Sharma, Comparative study of a three-bucket Savonius rotor with a combined three-bucket Savonius three-bladed Darrieus rotor, Journal of Renewable Energy, 2008; 33(9): 1974-1981.

[31] N.Fujisawa, F. Gotoh , Pressure measurements and flow visualization study of a Savonius rotor, J wind Eng Ind Aerodyn 1992;39:51-60. 32. Shankar PN. The effects of geometry and Reynolds number on Savonius type rotors. National Aeronautic Laboratory Bangalore 560017, AE-TM-3-76, 1976.

Nomenclature

C_d	: Drag Coefficient
C_p	: Power Coefficient
SIMPLE	Semi-Implicit Method for Pressure-Linked Equation
X	: Overlap
D	: Rotor Diameter
X/D	: Overlap ratio